Mask Pattern Recovery Using Level Set Method and its Application on Defect Auto Disposition based on Simulated Aerial/Wafer Image

Jin-Hyung Park[1], Paul.D.H Chung[1],Chan-Uk Jeon[1] and Han Ku Cho[1]
Photomask Team, Semiconductor R&D Center, Samsung Electronics Co., Ltd.
Banwol-Dong, Hwaseong-City, Gyeonggi-Do, Korea[1]

Linyong Pang[2], Danping Peng[2], Vikram Tolani[2], Tom Cecil[2], David Kim[2], KiHo Baik[2]
Luminescent Technologies, Inc. 2471 East Bayshore Road, Suite 600,
Palo Alto, CA 94303, USA[2]

ABSTRACT

At the most advanced technology nodes, such as 32nm and 22nm, aggressive OPC and Sub-Resolution Assist Features (SRAFs) are required. However, their use results in significantly increased mask complexity, making mask defect disposition more challenging than ever. This paper describes how mask patterns can first be recovered from the inspection images by applying patented algorithms that employ Level Set Methods. The mask pattern recovery step is followed by aerial/wafer image simulation, the results of which can be plugged into an automated mask defect disposition system based on aerial/wafer image. The disposition criteria are primarily based on wafer-plane CD variance. The system also connects to a post-OPC lithography verification tool that can provide gauges and CD specs, for use in mask defect disposition as well. Results on both programmed defects and production defects collected at Samsung's mask shop are presented which demonstrate the accuracy and consistency of using the Level Set Methods and aerial/wafer image based automated mask disposition.

Keywords: Mask inspection, mask pattern reconstruction, mask pattern recovery, mask pattern inversion, Inverse Lithography Technology (ILT), mask defect disposition, aerial image

1. INTRODUCTION

As semiconductor manufacturing processes advance in step with Moore's Law, the photomask industry has been increasingly challenged, especially as it entered the sub-wavelength era. When imaging at subwavelength, resolution enhancement technologies (RET) such as OPC, Phase Shift Masks (PSM), sub-resolution assist features (SRAFs), Source Mask Optimization (SMO), and Inverse Lithography Technology (ILT), are often required, adding complexity to the mask [1-8]. Figure 1 shows an example of how the use of ILT provides substantial increase in litho process window. However, in the process, the mask geometries and assist features, which play a crucial role in increasing the process window, also make the mask more complicated [8].

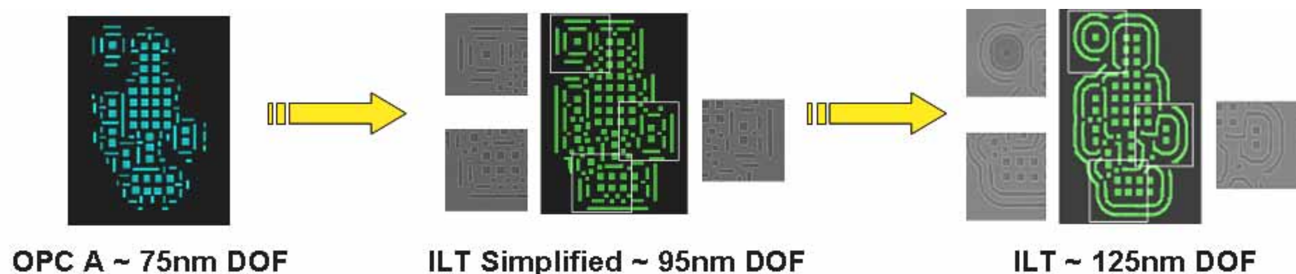

Figure 1: Trade-off between Inverse Lithography Mask Complexity and Lithographic Performance, PMJ 2009

	2009	2010	2011	2012	2013	2014
ITRS	52	45	40	36	32	28
SEC_DRAM	3X	2X	2X	1X	1X	1X
K1	0.24	0.20	0.16	0.49	0.39	0.31
SRAF	60	50	40	24		
Defect size	45	38	31	26	22	16
Sensitivity	40nm		30nm	22nm		18nm
Defect review	Optical tool(248)	Optical tool(193)				
	Optical simulator	Litho simulator using SEM and Inspection image				

Solution Exist | Risky Solution | No Solution

Figure 2: ITRS and Samsung roadmap

Figure 2 shows the ITRS and Samsung roadmap for mask inspection and defect disposition. While 248nm/193nm optical tools may be used to review defects post-inspection in the sub-3X node DRAM production, their use becomes limited when it is unknown how these defects really impact the intended main features that print. For example, mask patterns now substantially deviate from their target design and wafer images; the effect of phase defects seen on inspection images is different than its actual effect under print conditions; and because of varying MEEF between different geometries of the mask, the severity of mask defects no longer correlates with their size on the mask. To meet these challenges, mask inspection, review, and disposition increasingly rely on aerial image analysis.

Aerial images taken of mask patterns are closely representative of the intensity images of the same mask patterns on the scanner; thereby related to the actual wafer print CD. Hence, the Aerial Image Measurement System (AIMS^{TM}), which captures mask aerial images at the same wavelength and optical (NA/illumination/polarization) setup as the scanner illuminator, has become an essential tool for both pre- and post-repair mask defect review. Depending on the volume of defects captured during inspection, an AIMS system could be used to disposition all “real” defects detected, provided there is an automated way to consistently disposition the larger volume of AIMS data from all these defects. In the flow shown in Figure 3, instead of using an offline optic tool to further review “real” defects detected during inspection, the AIMS system together with SEM review of a subset of the OOS (Out-Of-Spec) defects is used.

However, due to the number of real defects detected during inspection and the throughput limitations of the AIMS tool, it may be impractical and is probably unnecessary to disposition every defect on the AIMS tool. Instead, an aerial-image based simulator could be used upstream after inspection, thereby lithographically filtering the bulk of the sub-specification defects, including inspection false defects or artifacts, leaving only marginal and lithographically significant defects for further AIMS disposition and repair. This requires a fast and accurate aerial image simulation from inspection images and an automated defect classification based aerial image to be developed.

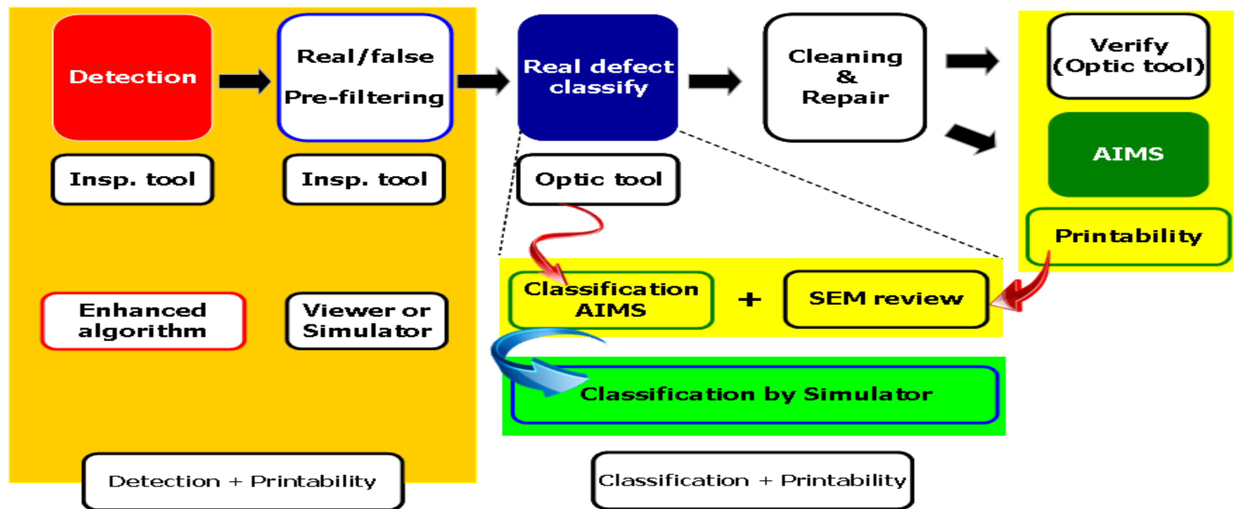

Figure 3: Samsung current and proposed mask defect disposition flows

2. LAIPH™ SOLUTION

Luminescent Automated Image Processing Hub (LAIPH™, pronounced "life") was developed to address the need discussed above. LAIPH includes integrated components that enable mask pattern recovery from non-actinic inspection images, as well as subsequent forward imaging of the recovered mask patterns to either wafer or AIMS optics, and finally automated dispositioning of defects in aerial images from these simulations, AIMS or even 193nm Aerial Plane Inspection Tool. Figure 4 shows the complete functionality of this hub.

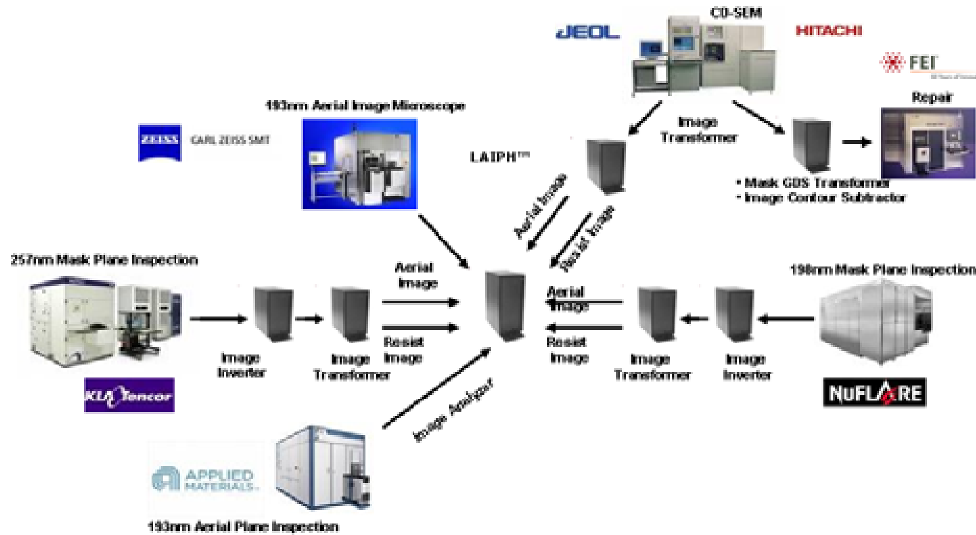

Figure 4: Luminescent Automated Image Process Hub (LAIPH)

An essential component of this hub which is required for any dispositioning is the capability to automatically disposition defects in aerial images. This disposition involves automatically aligning AIMS defect and reference images, computing AIMS reference image if one does not exist (for example in single die cases), calculating thresholds based on reference AIMS image and target design GDS, computing absolute and %CD change at the defective site, and then dispositioning the defects based on user-defined verification rules. Figure 5 shows how different topologies can be defined in order to apply different sensitivities not only to the current mask layer but also to the underlying and overlying mask layers[9].

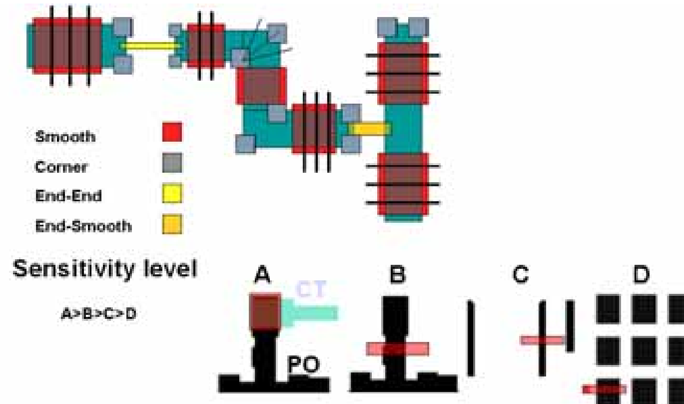

Figure 5: Topology based Multi-level Sensitivity & Defect Auto Classification

The specification of such critical markers, job management, review of output images, profiles, contours, etc. is enabled through intuitive web and native GUIs, a screen-shot of which is shown in Figure 6 below. All computations are carried out in a distributed computing environment providing a throughput that can be tailored to meet any realistic requirements (e.g., 1000 defects/minute).

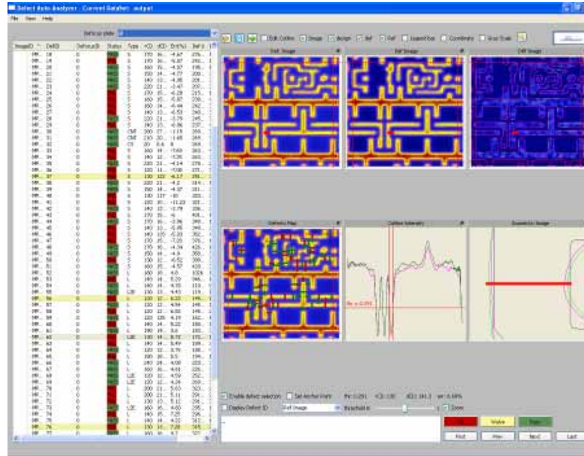

Figure 6: GUI for Automated Aerial Image disposition job management and review

The next key component of the LAIPH hub is the mask pattern recovery from an inspection image, for example from a KLA 5xx 257nm system. This recovery of the mask patterns is essential because at 3X node and below, mask GDS or SEM images look quite different than under the inspection tool optics. To address this problem of mask recovery, the same Level Set based algorithms that are used in Inverse Lithography Technology (ILT) to optimize mask patterns from intended wafer target are extended to recover the same mask patterns from their inspection optical image. Figure 7 shows how application of this method to two apparently similar inspection images yields quite different masks and their subsequent wafer aerial images.

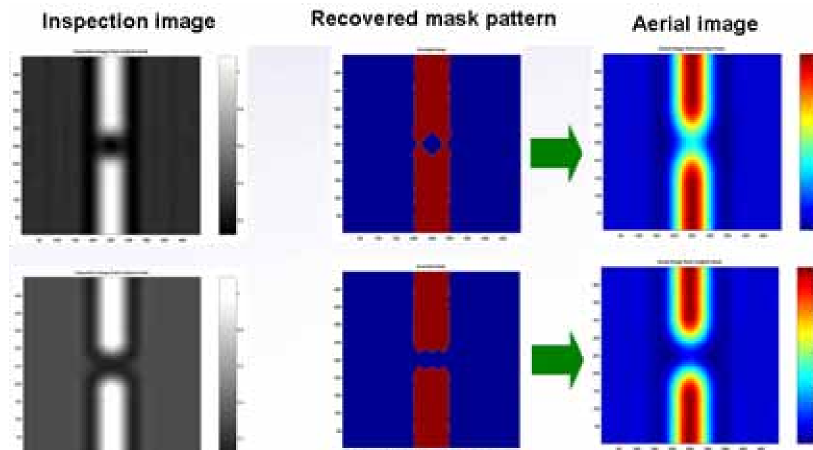

Figure 7: Similar mask inspection images may come from different defects

The accuracy and consistency of mask pattern recovery using this method is demonstrated on programmed defect masks first and then applied to production defects.

3. VALIDATION ON PROGRAMMED DEFECT MASK

A 5X node line/space programmed defect mask was designed with 6 types of programmed defects of increasing sizes. The mask was inspected on the KLA TeraScan^{TM} 257nm system with a pixel size of 90nm. The inspection defect and reference images were then run through the Level Set algorithms in the LAIPH system, the mask patterns were reconstructed and forward-simulated to emulate AIMS, and then automatically dispositioned to yield a defect CD delta value, as plotted in Figure 8 below. For comparison, the same defects were measured on the actual AIMS tool using the fast-scanner mode, which is intended to emulate full-vector effects. For consistency these AIMS images were also then dispositioned on the LAIPH and the defect CD delta values also reported in Figure 8a. As can be seen from the graph, the difference between the LAIPH simulated and actual AIMS measurements is < 3nm, with the variability of the AIMS system itself contributing ~1nm.

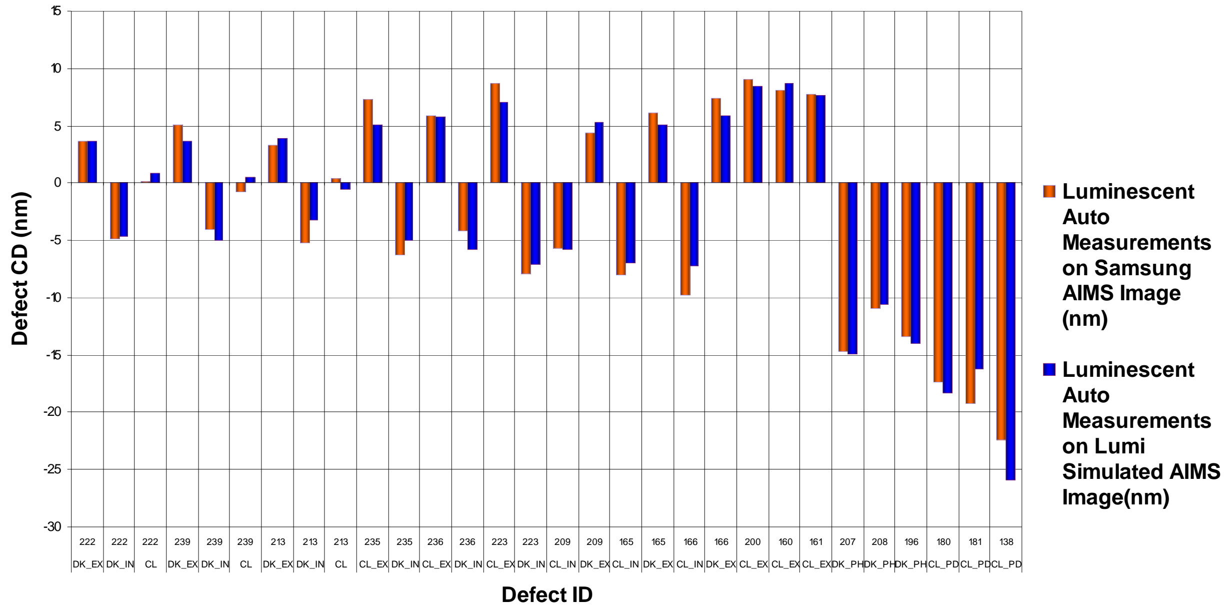

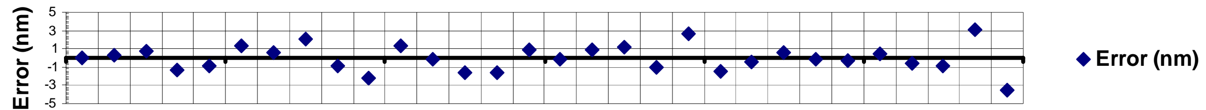

Figure 8a: Comparison of Defect CD on Aerial Image between Samsung AIMS and Luminescent Simulation

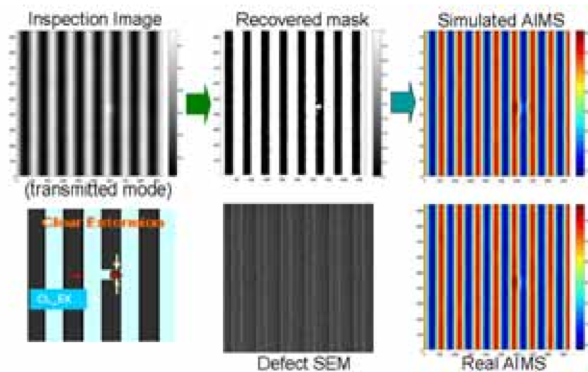

Figure 8b: 1st Butting (defect #213)

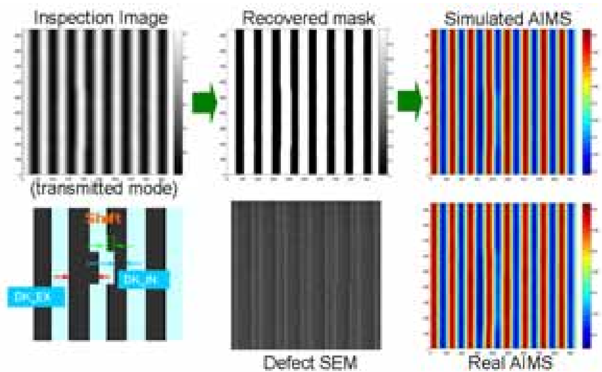

Figure 8c: 4th 2C-C (defect #161)

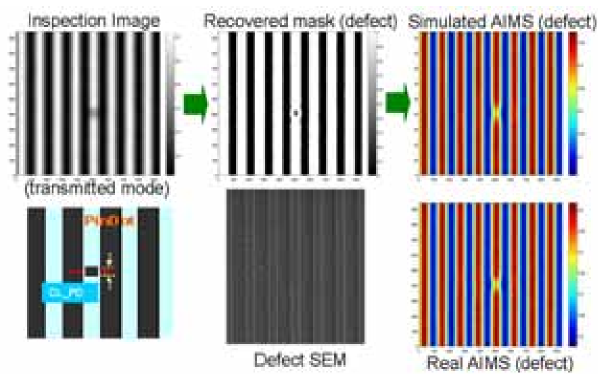

Figure 8d: 6th 2A (defect #196)

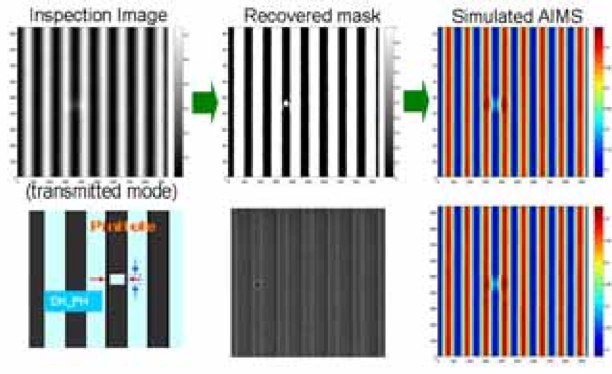

Figure 8e: 8th 1A (defect #138)

Figures 8b-8e show some sample cases, including the recovered masks and actual SEM images. A close match between the recovered masks and SEM images can be observed, validating the use of level set methods in mask pattern recovery. Furthermore, the close match between the simulated aerial image CD delta and actual AIMS measurements also shows that the simulations accurately capture the AIMS system model which has slight but crucial differences from the actual scanner optics, mainly in that it is a 450X magnification system instead of 0.25X reduction system. This will be further validated when applied to actual production mask defects.

As a means to understand the consistency of the automatically dispositioning aerial images on the LAIPH, these auto-measurements were compared to those measured manually by an AIMS operator (Figure 9). The variability in manual measurements is seen to be 3-4 times larger than measuring the same defects automatically in LAIPH. Hence the repeatability of dispositioning these defects is substantially improved when done in an automated procedure through LAIPH, thereby also lowering the precision/tolerance (P/T) of the measurement system as a whole.

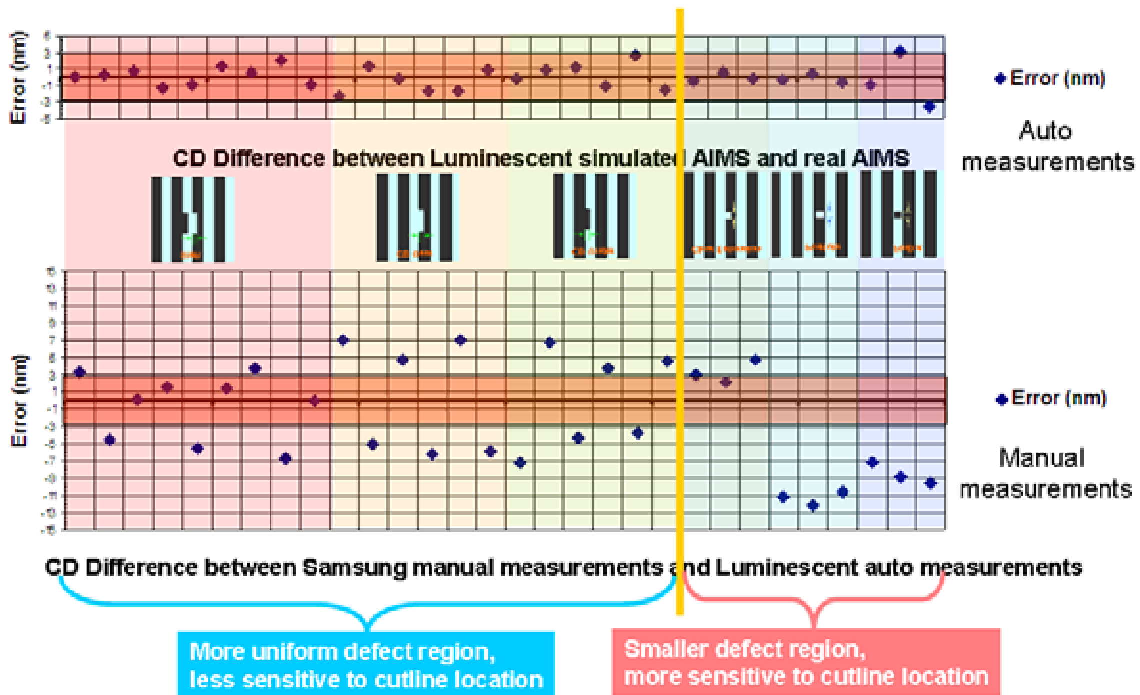

Figure 9: CD difference between Samsung manual measurements and LAIPH auto measurements

4. APPLICATION TO PRODUCTION MASK

A 5x node production mask layer with brick-wall patterns was inspected on the KLA TeraScan™ 257nm system with a pixel size of 72nm. A total of 293 defects were detected during this D:D inspection, most of which were in the critical end-to-end geometry. All these defects were run through the LAIPH system, and similar to the programmed defect mask case, corresponding defect and reference masks patterns were recovered and forward simulated to emulate AIMS, and then automatically dispositioned to yield the defect CD delta values. A sample of the significant defects was also measured on the AIMS tool. Figure 10 below shows the good matching between the AIMS tool profiles and contours and the corresponding simulated image. This represents a validation of the accuracy in modeling the inspection, AIMS, and reconstruction of the original mask itself.

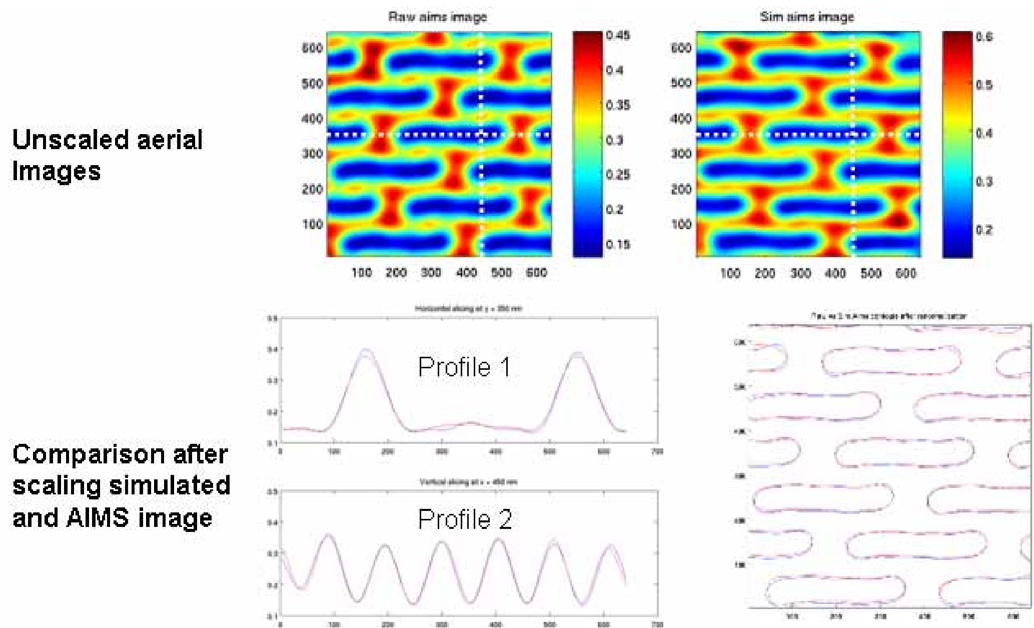

Figure 10: Overlaying actual AIMS and simulated AIMS horizontal/vertical profiles and Nominal contours

As a starting point, an 8%CD AIMS delta was assumed to separate defects into OOS vs. sub-spec. As can be seen in Figure 11, this results in 77 of the original 293 defects being OOS and thus needing further review or disposition. In the process, however, by using these simulations ~70% of the non-significant defects, including false and sub-specification defects, have been filtered out, thereby not requiring any review or repair.

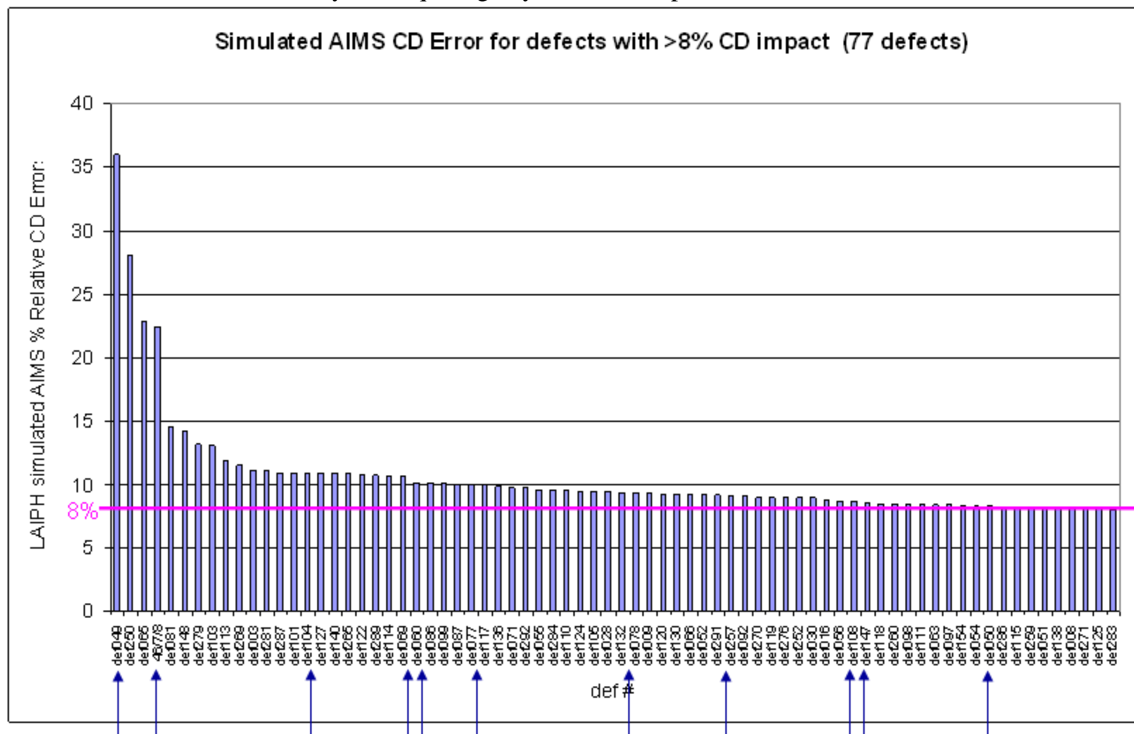

Figure 11: LAIPH simulated AIMS CD error, sorted in order of decreasing %CD error impact

Next, many of these defects that are OOS on aerial/wafer image may be difficult to identify and classify correctly by an operator based on visual review on the inspection or review tool. The difficulty in classifying these defects using their inspection images could be quantified in terms of intensity or CD differences between the inspection defect and reference image. When plotted against the corresponding the simulated AIMS CD error as shown in Figure 12, it can be seen that there are many defects with >8% AIMS CD error that have low inspection signal in terms of defect-reference intensity or CD difference and hence could be missed when manually classified by an operator. A sample of these defects is shown in Figure 13a-c. Figures 11-13 also show a cluster of the same effective defect #46-49 of most concern to Samsung and requiring repair.

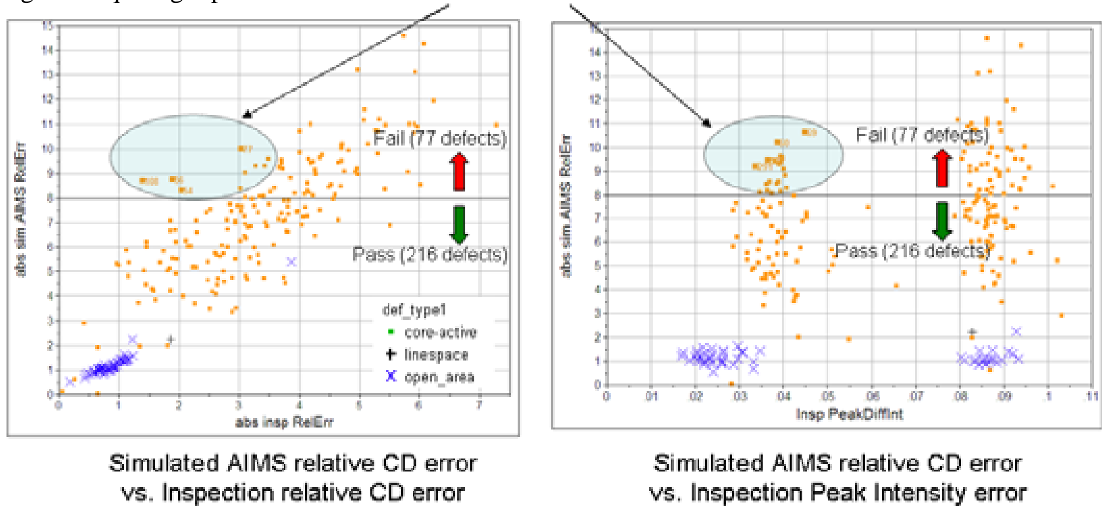

Figure 12: Aerial image plane simulations help to catch defects that could otherwise be missed during manual/visual classification by operator

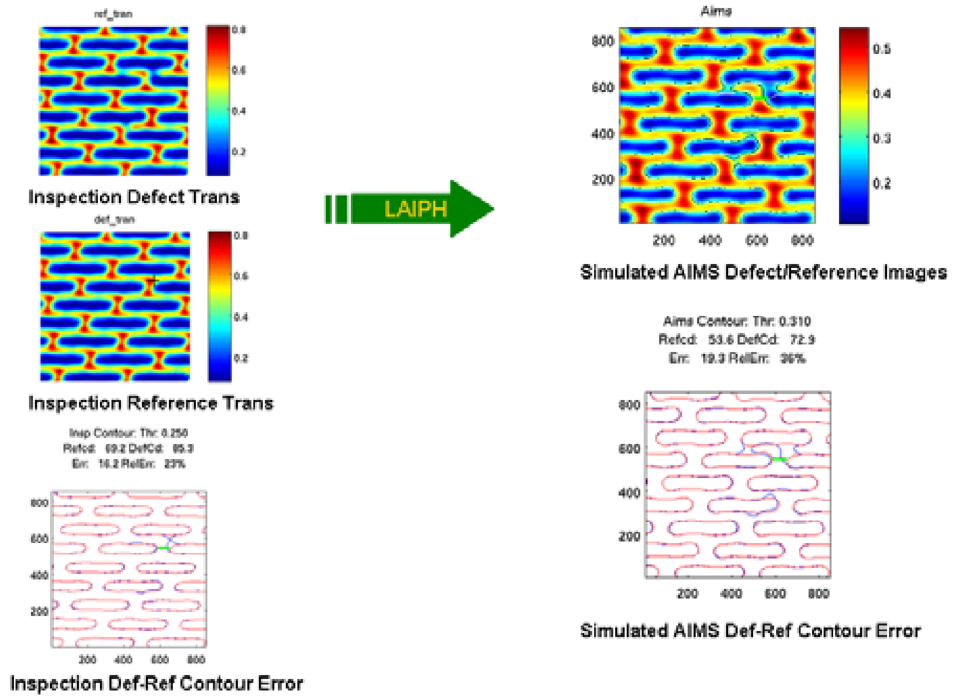

Figure 13a: Defect Review – def. #49 (largest defect)

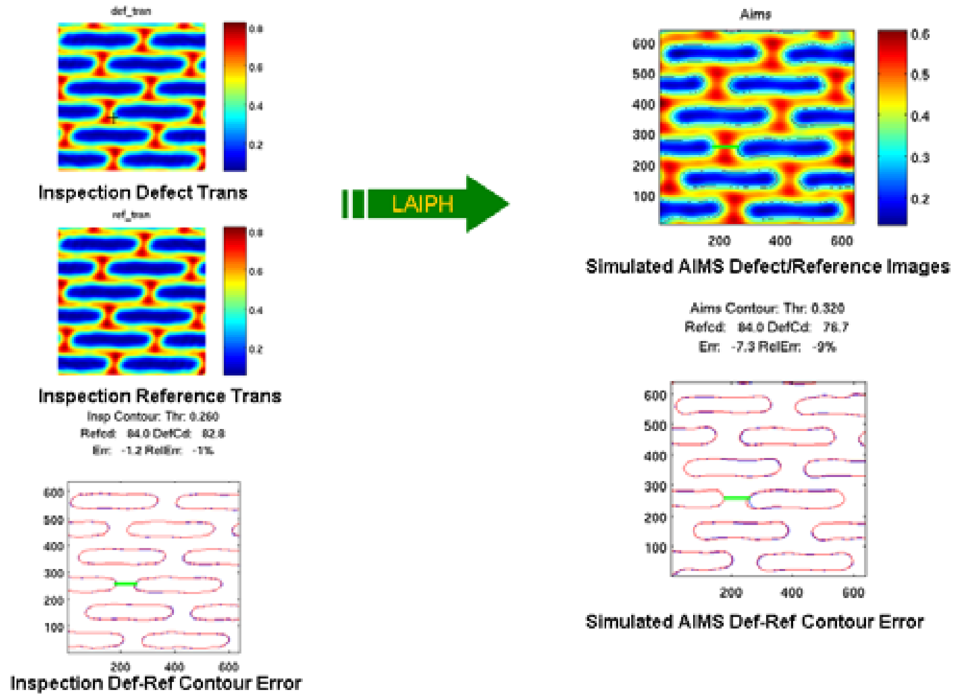

Figure 13b: Sample Defect Review – def. #108 (AIMS CD >> Insp. CD)

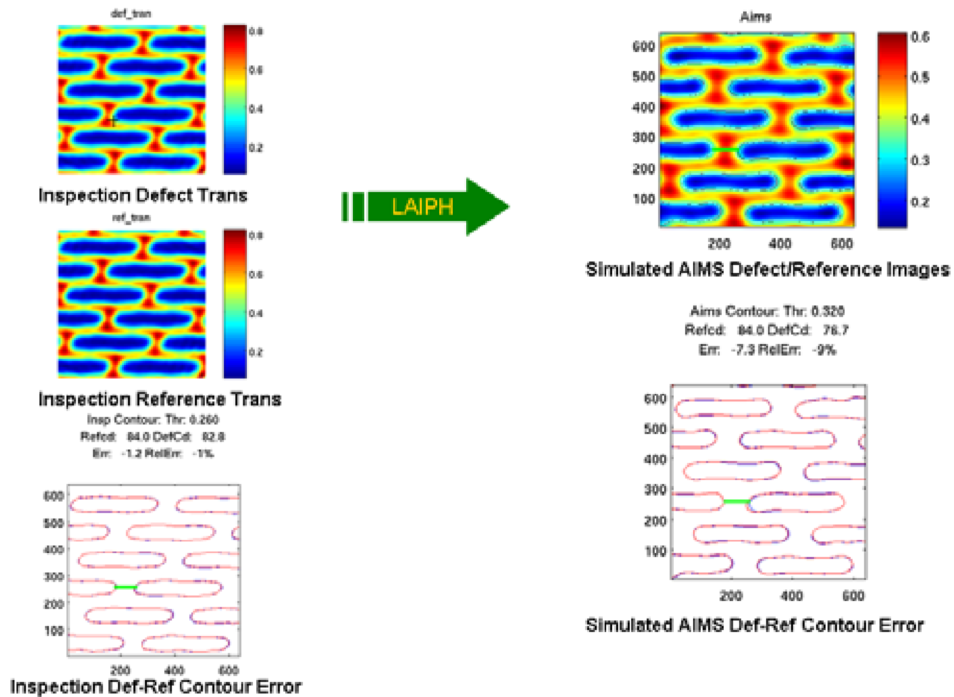

Figure 13c: Sample Defect Review – def. #60 (AIMS CD Hi >> Insp. Int. Lo)

5. CONCLUSIONS

As technology advances to 32nm, 22nm, and beyond, a paradigm shift is required in mask defect inspection and disposition: the manual defect classification based on mask image has to be replaced by defect printability based auto detection and classification; the review using optical image has to be replaced by AIMS and lithography simulations.

To achieve an accurate lithography simulation, the accurate mask pattern is essential. Mask pattern recovery based on level set methods using both transmitted and reflected image is very effective, particularly in recovering pin-hole and clear extension types of defects which are otherwise very difficult to recover through conventional inspection image processing techniques. From this study, it was demonstrated that the lithography simulation using the recovered mask pattern can achieve CD accuracy within ±3nm (including ±1nm variation due to AIMS) for all types of defects on the programmed defect mask for 5X node.

The auto CD measurement eliminates operator error and significantly improves the throughput. In this study, it is shown that CD measurement error is reduced 3~4X by using auto CD classification.

This study also demonstrates that aerial/wafer image based classification is able catch defects with higher MEEF values, which are difficult to identify by reviewing the mask inspection image alone. For the 5X node active layer production mask inspected on MPI 257, defects that could be difficult to classify/identify by operator during inspection review but still have significant litho impact were identified using the aerial image plane based defect classification and filtering.

6. FUTURE WORK

With EUV technology imminent in the near future and no EUV actinic inspection or AIMS tool development in the horizon, the level set method developed to reconstruct the mask from its non-actinic inspection image and forward image it to its correct litho conditions could be adapted to EUV mask defect disposition as well. This method of dispositioning could be supplemented with the use of SEM images of the defects as well.

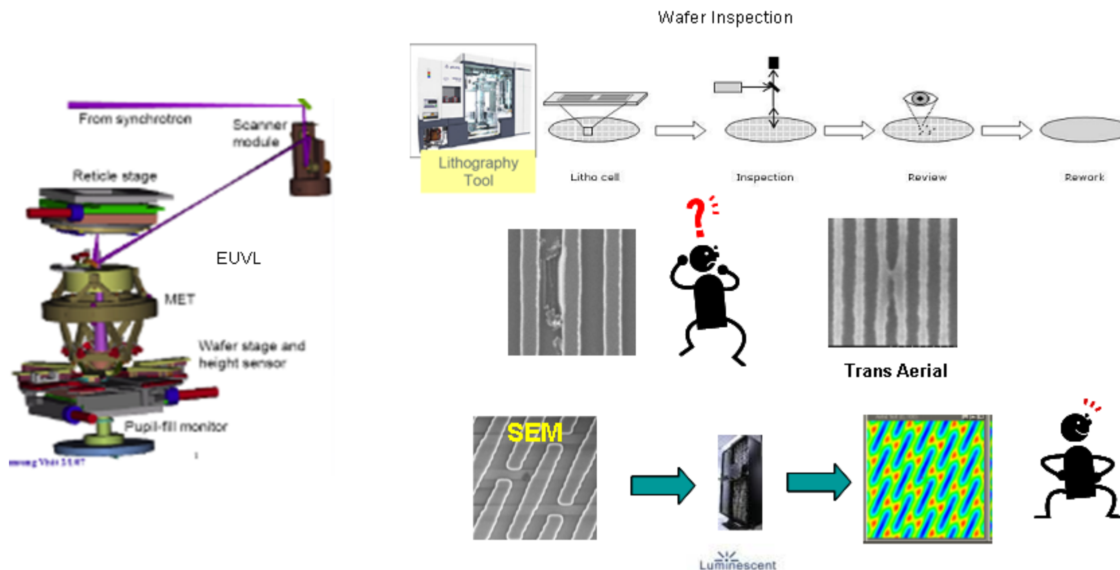

Figure 14: Future extension to EUV mask defect disposition

7. REFERENCES

[1] Abrams, S. and Pang, L., “Fast inverse lithography technology”, 31st Internal Symposium of Microlithography, Proc. SPIE 6154 (2006).

[2] Pang, L., et al, "Inverse Lithography Technology (ILT), What is the Impact to Photomask Industry?", Proc. SPIE 6283, (2006)

[3] Pang, L., et al, "Inverse Lithography Technology (ILT): Keep the balance between SRAF and MRC at 45and 32 - nm", Proc. SPIE 6730, (2007)

[4] Pang, L., et al, " Validation of Inverse Lithography Technology (ILT) and Its Adaptive SRAF at Advanced Technology Nodes ", Proc. SPIE 6924, (2008)

[5] Prins, S. L., et al, "Inverse Lithography as a DFM Tool: Accelerating Design Rule Development with Model-Based Assist Feature Placement, Fast Optical Proximity Correction and Lithographic Hotspot Detection", Proc. SPIE 6924, (2008)

[6] Xiao, G., et al, " Source Optimization and Mask Design to Minimize MEEF in Low K1 Lithography", Proc. SPIE 7028, (2008)

[7] Maurer, W., “Mask specifications for 193 nm lithography,” 16th Annual BACUS Symposium on Photomask Technology and Management, Proc. SPIE 2884, 562-571 (1996)

[8] Kim, B.G., Suh S.S., Kim B.S., Tolani, V., Dai G., Irby D., Wang K., Xiao G., Kim, D., Baik K., and Gleason, B., “Trade-off between Inverse Lithography Mask Complexity and Lithographic Performance “, JPM09-7379-57 (2009).

[9] Chen, C. Y. et al, “ Mask defect auto disposition based on aerial image in mask product”, Proc. SPIE 7379, 73791F (2009)